Superconducting Tunnel Junctions As Detectors For Ultraviolet,Optical, and Near Infrared Astronomy.

Tone Peacock, P. Verhoeve, N. Rando,
M.A.C. Perryman, B.G. Taylor, P. Jakobsen

Astrophysics Division, Space Science Department of the European Space Agency, ESTEC, Noordwijk, 2200 AG, The Netherlands.

ESLAB 96/151

Astrophysics Division - Space Science Department

European Space Agency
Agence spatiale européenne

ESTEC

A&A manuscript no.
(will be inserted by hand later)

Your thesaurus codes are:
03.09.1; 03.09.6; 03.20.4

ASTRONOMY
AND
ASTROPHYSICS
28.7.1996

Superconducting Tunnel Junctions as Detectors for Ultraviolet, Optical, and Near Infrared Astronomy

Tone Peacock, P. Verhoeve, N. Rando, M.A.C. Perryman, B.G. Taylor, P. Jakobsen

Astrophysics Division, Space Science Department of ESA, ESTEC, Noordwijk 2200AG, The Netherlands

Received:

Abstract. We discuss the capabilities of superconducting tunnel junctions as detectors for ultraviolet, optical, and near-infrared astronomy. Such junctions have recently been shown to allow the detection of individual optical and ultraviolet photons with an inherent spectral resolution related to the critical temperature of the absorbing superconductor. Limiting resolutions at 500 nm ranging from 5–40 nm (for materials with critical temperatures between 0.1 to 10 K) should be achievable. These detectors should have a high quantum efficiency (> 50 per cent) over a very broad wavelength range from the ultraviolet to the near infrared (100–2000 nm). The overall efficiency is limited by reflection from the superconducting film, and should be improved significantly by appropriate anti-reflection coatings. The devices function at very high incident photon rates—with count rates of order 10 kHz or higher being feasible, and photon arrival time datation possible to microsec-level accuracy. It is realistic in the future to envisage that these devices, of a size typically $20 - 50\mu m^2$, could be packaged into imaging arrays. These key characteristics imply that many areas of optical and ultraviolet astronomy could benefit significantly from their further development.

Key words: Instrumentation: detectors – photometry – superconductors – tunnel junctions – optical/ultraviolet spectroscopy

1. Introduction

The ideal detector for application in a variety of astronomical studies at ultraviolet, optical, and infrared wavelengths is one which can simultaneously over a wide waveband provide the wavelength, time of arrival and location of each photon falling upon the detector from the widest possible field. Intrinsic energy discrimination, although typical of modern X-ray detectors such as X-ray CCDs, does not occur in any existing ultraviolet or optical detector systems. Any detector development which provides these key features will make a major contribution to astrophysical research by improving the sensitivity limits for faint object spectroscopy, and by simultaneously providing the photon arrival time.

Perryman, Foden & Peacock (1993) proposed, largely on theoretical grounds, that optical detectors based on superconductors could make a major advance in the development of instrumentation for application in astronomy. Since this proposal experimental demonstration of the basic principles using niobium-based superconductors by Peacock et al. (1996a, b) has shown the validity of this approach. In this paper we extend these initial ideas to the more general case of an arbitrary superconductor, consider the effects of multiple tunnelling, and indicate the wavelength resolution that may ultimately be expected under various conditions.

Despite the considerable strengths which have made the CCD the pre-eminent detector for optical astronomy, three performance weaknesses still exist: the lack of an inherent spectral resolution, the limited quantum efficiency at short wavelengths (in the blue/ultraviolet), and the inability to photon count—and thereby provide the arrival time of the incident photon (Delamere 1992). Current photon counting detectors cannot compete with CCDs except with respect to time resolution, and for applications involving very low signal levels. None provides a measure of the photon wavelength, all have a limited quantum efficiency due to the available photocathode materials, and all are limited by their photon count rates (Timothy 1988, Petroff & Stapelbroeck 1989). Photon-counting ability has potential applications in many fields of astronomy, e.g. the study of the optical properties of variable sources, as well as compensation for the effects of atmospheric seeing. It is however the lack of any intrinsic wavelength discrimination which is a serious limitation of all available photon detectors, and which the superconducting detector overcomes for the first time.

Detectors based on semiconductors have a bandgap (1.1 eV for silicon) of order of the (optical) photon energy. Photoabsorption results in typically only one electron being excited from the valence to the conduction band, irrespective of photon wavelength. This precludes, without some form of amplification, the possibilities of photon counting, and/or wavelength discrimination.

This is not however the case for superconductors. As broad-band, noiseless, high speed photon counting detectors,

with inherent spectroscopic ability—and thus the ability to cover efficiently in a single detector the waveband from the ultraviolet to the near infrared with medium spectroscopic resolution—they could allow developments in a number of different fields of astronomy. For example the observation of emission-line complexes or continuum absorption features such as the Lyman edge in very faint extragalactic objects may allow the direct determination of their red shifts. Applications requiring time resolution, either to measure intrinsic variability characteristics (e.g. Dravins 1994) or to overcome atmospheric effects, will also become more accessible.

2. The Photoabsorption Process in Superconductors

As identified by Perryman, Foden & Peacock (1993) optical detectors based on superconducting materials offer two important advantages over those based on semiconductors: (a) according to the BCS theory of superconductivity the energy gap Δ between the ground state, as represented by the bound Cooper pairs, and the first excited state, containing the broken Cooper pairs known as 'quasiparticles', is generally more than 10^3 times smaller than the energy gap between the valence and conduction bands of a semiconductor (Bardeen, Cooper & Schrieffer, 1957); (b) the Debye energy Ω_D is much larger than the superconducting energy gap, thereby allowing phonons created as a result of the photoabsorption process to break Cooper pairs and create free charge (Wood & White 1969). For example in bulk Al $\Delta \sim 170\mu$eV while Ω_D is as large as ~ 37 meV.

In a superconductor the conduction electrons at a particular transition temperature interact with the lattice (an attractive electron-phonon interaction) which overcomes their mutual Coulomb repulsion leading to the formation of electron pairs. It is these Cooper pairs which carry the electrical current. The temperature at which the phase transition occurs, when electrons begin to form into condensates of pairs, is known as the critical temperature T_c. The Debye energy can be interpreted here as the maximum energy associated with the vibrational modes of the lattice. Table 1 summarises some of the key parameters of some elemental superconductors.

At sufficiently low temperature (typically about an order of magnitude lower than the superconductor's critical temperature T_c) the initial number of quasiparticles N_0 created as a result of the absorption of a photon of wavelength λ, can be in excess of any thermally induced population and is inversely proportional to the photon wavelength λ. In general, N_0 can be written:

$$N_0(\lambda) \sim 7 \times 10^5/\lambda\Delta(T) \quad (1)$$

where $\Delta(T)$ is the temperature-dependent energy gap. The mean energy, ϵ, required to create a single quasiparticle in Nb and Sn has been calculated to be $\sim 1.75\Delta$ and $\sim 1.7\Delta$ respectively (Kurakado 1982, Rando et al. 1992). The variance

Table 1. Basic parameters of some elemental superconductors. T_c is the critical temperature, Ω_D the Debye energy, and Δ the energy gap. H_c is the critical magnetic field above which the superconducting state of the material is either destroyed or modified.

Material	T_c (K)	Ω_D (meV)	Δ (meV)	H_c (G)
Niobium	9.20	23.7	1.550	1980
Vanadium	5.30	32.7	0.800	1420
Tantalum	4.48	20.7	0.664	830
Aluminium	1.14	36.9	0.172	105
Molybdenum	0.92	38.8	0.139	95
Cadmium	0.56	18.0	0.083	30
Titanium	0.39	36.2	0.059	100
Hafnium	0.13	21.7	0.020	13

on $N_0(\lambda)$ defines the fundamental limit to the intrinsic resolution $d\lambda_F$ of the superconductor. This limiting resolution, known as the Fano-limit, can be written as:

$$d\lambda_F \sim 2.8 \times 10^{-3}\lambda^{3/2}[F\Delta(T)]^{1/2} \quad (2)$$

where, in both equations, the bandgap Δ is in meV and λ is in nm. F is the Fano factor (Fano 1947) which has been shown to be ~ 0.22 and ~ 0.19 for Nb and Sn respectively (Kurakado 1982, Rando et al. 1992). The values $\epsilon \sim 1.75\Delta$ and $F \sim 0.2$ can be considered as typical of many of the elemental superconductors.

In superconductors such as Nb or Al operating at $\sim 0.1\,T_c$, with critical temperatures of 9.2 and 1.14 K respectively, the initial charge $N_0(\lambda)$ created by the photoabsorption of an optical photon with $\lambda = 500$ nm is of order 10^3 and 10^4 quasiparticles respectively. The corresponding Fano-limited wavelength resolution in Nb or Al is ~ 17 nm and ~ 4 nm respectively.

Equations 1 and 2 can be further generalised to any superconductor through use of the approximate BCS relation in the weak coupling limit which links the bandgap at absolute zero to its T_c such that $\Delta \sim 1.75kT_c$, where k is Boltzmann's constant (for a strongly-coupled superconductor such as Nb, a somewhat better approximation is $\Delta \sim 1.93kT_c$) giving:

$$N_0(\lambda) \sim 4.6 \times 10^6\lambda^{-1}T_C^{-1} \quad (3)$$

$$d\lambda_F(\text{nm}) \sim 5 \times 10^{-4}\lambda^{3/2}T_c^{1/2} \quad (4)$$

Figure 1 illustrates this fundamental limiting spectral resolution $d\lambda_F$ for a number of elemental superconductors. For Al the resolution between Lyman-α ($\lambda = 121.6$ nm) and $\lambda \sim 2\mu$m ranges from ~ 0.7 to 50 nm respectively, with $N_0(\lambda)$ ranging from $\sim 3 \times 10^4$ to $\sim 2 \times 10^3$. If a low T_c superconductor such as Hf were used, the Fano-limited resolution would, over the same wavelength band, range from 0.2 to 15 nm.

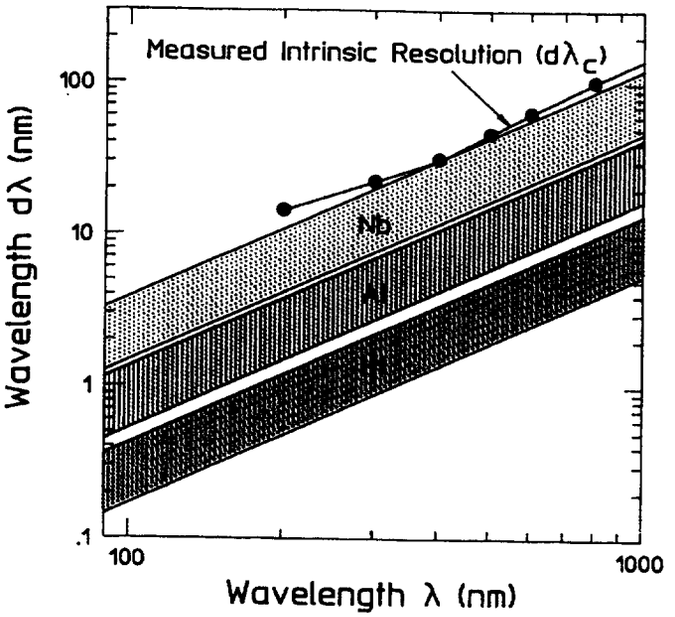

Fig. 1. The Fano and tunnel noise-limited resolution, $d\lambda_F$ and $d\lambda_T$ (lower and upper sloping lines respectively), versus wavelength for three superconducting materials. The electronics-corrected measured resolution $d\lambda_e$ (nm) for a Nb-based symmetrical junction is also shown. The shaded regions indicate the range of possible resolutions $d\lambda_F$ to $d\lambda_T$ which will depend on the design of the STJ and the role of multiple tunnelling (Section 3.2).

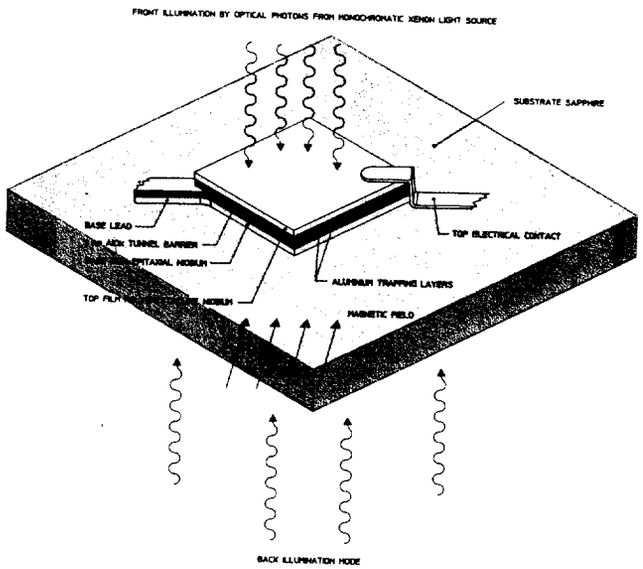

Fig. 2. A schematic of a typical symmetrical tunnel junction deposited on a sapphire substrate together with its orientation in a parallel magnetic field so as to suppress the Josephson current. Such a device was used by Peacock et al. (1996 a, b) to demonstrate single photon counting from 200–550 nm. Back or front illumination is possible.

3. The Superconducting Tunnel Junction

3.1. Principles of Operation

One of a number of ways of detecting the excess quasiparticles produced as a result of the photoabsorption process is by ensuring that they tunnel from one thin superconducting film (S_1) in which they are created into another (S_2) through a thin insulator (I). To maximise the tunnel probability this insulating barrier must be very thin, of order 1 nm (i.e. only a few atomic layers). This superconductor-insulator-superconductor (or SIS) structure is in essence a superconducting tunnel junction (STJ) or Josephson junction (Giaever 1960, Josephson 1962). A small magnetic field is applied parallel to the junction barrier, as shown in Figure 2, so as to suppress the Josephson current which results from the tunnelling of Cooper pairs at zero bias voltage. Applying a bias voltage $V_b < 2\Delta/e$ ensures that the only allowed tunnel processes involve the transfer of quasiparticles from one film to the other. The flow of quasiparticles in a time t produces a measurable excess electric current, with the amplitude of the current pulse being directly proportional to the incident photon energy.

3.2. Multiple Tunnelling and Tunnel Noise

For the case where $V_b < 2\Delta/e$ two tunnel processes exist (Gray 1978). In the first process an electron tunnels from film S_1 to film S_2 (the direction depends simply on the polarity of V_b) and effectively a quasiparticle is exchanged, while in the second process an electron tunnels again from film S_1 to S_2 while a quasiparticle is exchanged between films S_2 and S_1. The combination of these two processes in series leads to an effect known as multiple tunnelling, which can be viewed as equivalent to an amplification of the initial charge $Q_0^i = eN_0^i(\lambda)$ created in the superconducting film i. If each quasiparticle originally created in the film is transferred across the barrier on average of n times then, in the absence of loss processes, the average total electrical charge detected would be nQ_0^i. In this time-dependent process, recombination, diffusion losses and quasiparticle trapping will all reduce $Q_0^i(t)$ (Booth 1987, Verhoeve et al. 1996).

This charge amplification will however degrade the Fano-limited resolution of the STJ by adding in quadrature the variance on this tunnel process, a contribution referred to as the tunnel noise (Goldie et al. 1994). On the assumption of a perfectly symmetrical junction (with equal probabilities of tunnelling from S_1 to S_2 and from S_2 to S_1) the resolution is given by:

$$d\lambda_T(\text{nm}) \sim 1.1 \times 10^{-3}\lambda^{3/2}T_c^{1/2}[F + \frac{n+1}{n}]^{1/2}, \quad n \geq 2 \quad (5)$$

This limiting resolution for a perfectly symmetrical STJ is also shown in Figure 1 for the case $n = 5$. This choice of n is based on the experimental determination by Peacock et al. (1996a) for a symmetrical Nb-based device. Figure 1 shows that a resolution of $\sim$ 40 nm and $\sim$ 14 nm is achievable for simple Nb and Al based devices respectively when illuminated by photons of wavelength $\lambda \sim 500$ nm. The degradation due to an equivalent amplification through multiple tunnelling is

not a basic limitation, since the need for such amplification is dependent on the signal-to-noise ratio and hence on the noise of the readout electronics. Provided the initial charge is sufficiently large compared to the electronic noise then such an amplification is not essential, and the contribution of the tunnel noise to the overall resolution can be reduced. Naturally, this requirement affects the basic design of the STJ and, depending on the materials used, its operating temperature. For these reasons we show the limiting resolution in Figure 1 as a band ranging from $d\lambda_F$ to $d\lambda_T$, for the case $n \sim 5$.

Effects of the quasiparticle lifetime and the role of various recombination mechanisms were considered by Perryman, Foden & Peacock (1993). For a typical $20 \times 20\mu m^2$ device with a film thickness of 100 nm, i.e. a film volume $V \sim 40\mu m^3$, the number of thermal quasiparticles can be written:

$$N_T \sim 2N(0)V(2\pi\Delta kT)^{1/2}e^{-\Delta/kT} \quad (6)$$

where $N(0)$ is the single spin electronic density of states at the Fermi energy. From equation (3) a photon of wavelength 500 nm will produce an initial number of quasiparticles N_0 of order 10^3, 10^4 and 10^5 for Nb, Al and Hf respectively. Combining equations (3) and (6):

$$N_0/N_T = 1.4 \times 10^{10} T_c^{-3/2}(\lambda N(0)V)^{-1}T^{-1/2}e^{1.75T/T_c} \quad (7)$$

It is reasonable to require that the thermal population is at least an order of magnitude lower than $N_0(\lambda)$. This means that, in the absence of additional barrier leakage mechanisms (thermal regime), the operating temperature T has to be less than $\sim 0.1T_c$, $0.15T_c$ and $0.24T_c$ for Nb, Al and Hf respectively (i.e. $\sim$ 900, 170 or 30 mK) to detect 500 nm photons. In the event of multiple tunnelling, these requirements may be somewhat modified.

3.3. Photon Detection at Optical Wavelengths

The superconducting tunnel junction has been extensively investigated as a photon detector in the X-ray region of the spectrum where the number of quasiparticles generated after photoabsorption are $\sim 10^3$ times larger than in the optical.

Peacock at al. (1996a, b) have recently reported the first experimental demonstration of photon counting at optical and ultraviolet wavelengths using an STJ. Single photon spectra from monochromated ultraviolet and optical photons covering the waveband 200–500 nm were obtained by illuminating a $20 \times 20\mu m^2$ device. This symmetrical device, which was constructed of aluminium-proximised niobium layers [Nb–Al] ($\Delta \sim 0.5$ meV) operated at a temperature of 0.4 K, is shown schematically in Figure 2. After removal of the contribution to the resolution from electronic noise a device-limited resolution $d\lambda_c$ was derived. Spatial variations in the response of the detector, similar to those reported by Verhoeve et al. (1996) and Lumb et al. (1995) at X-ray wavelengths, may account for the small degradation in resolution compared with that expected theoretically.

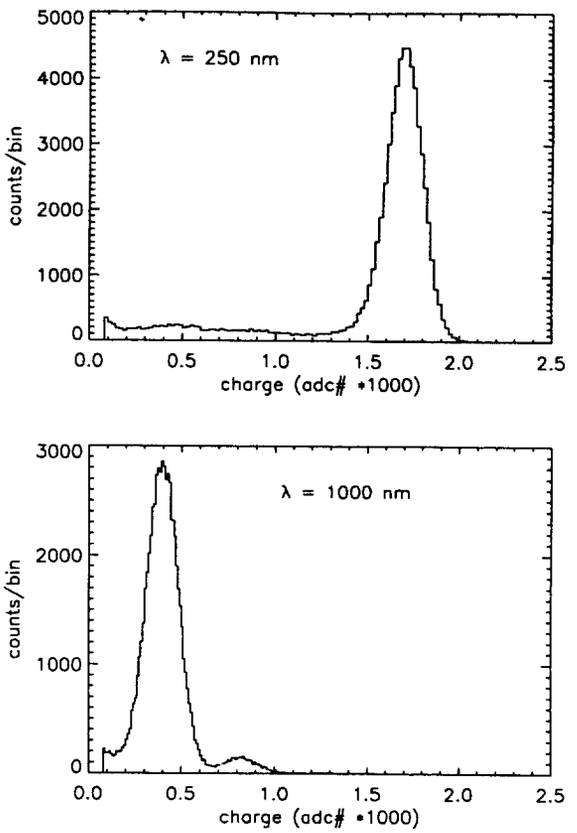

Fig. 3. Single photon charge spectrum of the device (a histogram of the number of photons giving a charge output Q from the detector) when illuminated by a monochromatic source of photons of wavelength 250 nm (top) and 1000 nm (bottom). The charge is in arbitrary units. The difference in the charge output versus wavelength provides the intrinsic energy resolution.

Recent performance improvements have been brought about by reducing the noise associated with the electronics, and by back illumination through the sapphire substrate onto the high quality epitaxial Nb film (cf. Figure 2), leading to a wavelength coverage extended to 200–1000 nm (the short wavelength limit is simply limited by the experimental conditions). The device-limited resolution $d\lambda_c$ is shown in Figure 1 for this Nb-based device. A resolution $d\lambda_c$ of 45 nm at $\sim$ 500 nm was obtained, very close to the theoretical value $d\lambda_T$ for Nb shown in Figure 1.

Figure 3 illustrates the single photon charge spectra, Q, obtained from this Nb device when illuminated with photons having a wavelength of 250 and 1000 nm.

4. Performance Capability

4.1. Absorption Efficiency and Reflectivity

The STJ has a very high efficiency to the absorption of photons of wavelength ranging from the ultraviolet to the near infrared. Figure 4(a) illustrates the absorption efficiency for single photons in Nb, Al and Hf films of thickness 100 nm

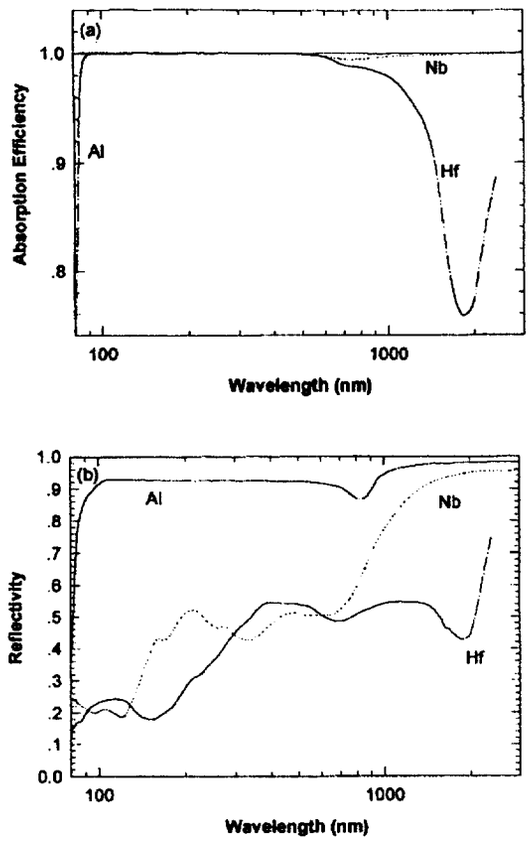

Fig. 4. The theoretical absorption efficiency, $A(\lambda)$ (a) and surface reflectivity $R(\lambda)$ (b) in a 100 nm film as a function of photon wavelength for Nb, Al and Hf. The reflectivity can be further decreased through the use of an anti-reflection coating at the expense of reducing the wavelength coverage. The overall quantum efficiency of the device for the case of front illumination is $A(\lambda) \times (1 - R(\lambda))$.

based on the optical constants of the materials (Weaver & Lynch 1973, Weaver et al. 1981) and indirectly confirmed for Nb-based devices through optical transmission measurements in our laboratory. From 100 nm to 2 μm the absorption efficiency is over 80 per cent for all three materials. The surface reflectivity of these films is shown in Figure 4(b). While pure Al has a very high reflectivity from the ultraviolet to the near infrared, typically over 90 per cent, the other two superconductors in Figure 4(b) have a much improved capability. Hf in particular has a reflectivity below 30 per cent in the ultraviolet and maintains a value below 55 per cent out to 2 μm. For Nb, where an optically-sensitive STJ now exists, the reflectivity is below 50 per cent out to 700 nm. The reflectivity, which affects not only the superconducting thin film but, depending on the mode of illumination (front illumination directly onto the top polycrystalline superconducting film or back illumination through the substrate onto the epitaxial base film), also the substrate, and substrate to base film interface, can be reduced through the use of anti-reflection coatings, albeit at the expense of bandwidth and with device fabrication constraints. Such coatings are currently under development.

Further reduction in the electronic noise should lead to resolutions approaching the theoretical limits shown in Figure 1. The resulting spectroscopic performance is illustrated in Figure 5 ($N \sim 5$) applied to emission line spectra from neutral (I) to quadruply ionised (V) atoms of oxygen and carbon. The line strengths (not corrected for abundances) and wavelengths are taken from Weast (1981). For the ion species III–V the line strengths should be considered as qualitative estimates of the relative strengths between different lines from the same atom. The intensity of the ionised atoms (II–V) relative to the neutral atom evidently depends on the excitation conditions. Figure 5 demonstrates that even the Nb device has a significant spectroscopic capability with many of the key lines of astrophysical interest being clearly resolvable.

The reflectivity of Al junctions is so high that the overall efficiency would limit considerably its usefulness at these wavelengths. While no devices based solely on Hf yet exist, it has formed the basis for some tunnel junction work (Morohashi et al. 1992). Nb- and Ta-based devices are however more standard, requiring only some improvements to achieve the theoretical limited resolutions of Figure 1. From Figure 5 however it is clear that an excellent spectroscopic capability would exist for devices based on Hf, with key transitions from the same ion as well as different ionic species being possible to resolve and identify.

4.2. Count Rates

Another significant strength of superconducting tunnel junctions is the inherent speed of the device. The time taken to complete the full conversion of the photon energy into quasiparticles, including their relaxation down to an energy equal to the bandgap of the absorbing material, is only a few ns. The quasiparticle confinement time in the film is complex and depends also on the superconducting material properties, bias voltage and film thickness. Based on the work of de Korte (1992) the confinement time in a single film can be written:

$$\tau_{\mathrm{tun},i} = 4e^2 N(0) V_i R_N \frac{[(\Delta_i + eV_b)^2 - \Delta_i^2]^{1/2}}{(\Delta_i + eV_b)} \qquad (8)$$

where $N(0)$ is the single spin electronic density of states at the Fermi energy, e the electron charge, R_N is the normal state barrier resistance, V_i is the volume of the film i and V_b is the bias voltage applied across the two films. Thus for a device designed to provide a single tunnel from a 100 nm thick film of Nb across a barrier having a typical resistivity $\rho \sim 2.5 \times 10^{-6} \Omega\,\mathrm{cm}^2$, the average confinement time is of order 100 ns, scaling with the mean number of transfers n across the barrier. The parameter $n\tau$ therefore represents approximately the intrinsic time resolution of the device.

Thus, in theory, superconducting tunnel junctions could be operated as photon counting detectors at rates of order 10^5 to 10^6 Hz depending on the device geometry and n. In practice Lumb et al. (1995) have shown rates as high as $\sim$ 7.5 kHz can be achieved without any intrinsic spectroscopic degradation in the device, being limited by the processing speed of the

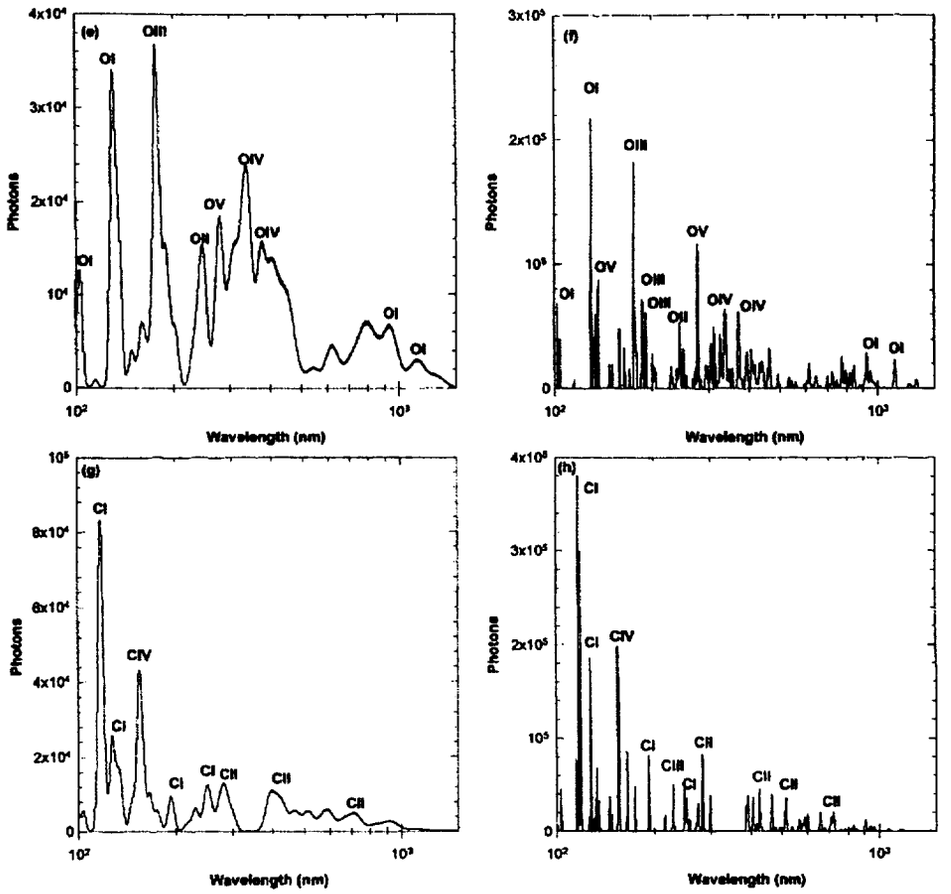

Fig. 5. The simulated tunnel-limited response $d\lambda_T$ ($n \sim 5$) from either a pure Nb based STJ (left two diagrams) or Hf based STJ (right two diagrams) to the principle emission lines from oxygen (top pair) and carbon (bottom pair). The strongest lines from neutral and ionised species are marked. Note the photon scale is different in each case to highlight the various line features. For all these spectra the bin size was set at 0.1 nm. No abundances are included in these simulations.

analogue electronics and substrate noise associated with the X-ray photon energy used in the experiment. The electronics however will be the final limitation to the very important photon count rate capability at optical wavelengths. These rates will still allow very high speed photometry on objects to be limited primarily by the collecting aperture of the telescope as well as the observation of fields containing a objects having a wide dynamic range in intensity.

Since each photon results in an electrical pulse whose amplitude is directly proportional to the photon energy, and a pulse risetime which is characteristic of a single photoabsorption event in the film, the device has intrinsic background rejection capabilities. Background from cosmic rays can be vetoed either by an upper energy threshold discriminator or through the risetime signature.

For a panoramic imaging STJ camera covering a wide field of view a number of approaches can be considered. It must however be noted that each STJ detector is independent and requires its own analogue electronics chain including the preamplifier. This is a considerable limitation, the solution to which still needs to be fully addressed. Nevertheless, simple limited close-packed arrays of 6×6 STJs are already under development by our group (Rando et al. 1996), while Perryman et al. (1993) already proposed more complex schemes in an attempt to reduce the total number of detectors and associated electronic chains while maintaining field coverage.

Although the count rates that can be handled in photon counting mode are already expected to be very high, there may be applications (for example, at longer wavelengths, for very bright objects, or for large telescope apertures) where even these limits are exceeded. Under these conditions, it is likely that the relevant junctions can be read out in an analogue mode, in which the steady-state current is measured, rather than the pulse corresponding to an individual photon. In these circumstances, the STJ would simply provide the total energy incident on the junction, integrated over wavelength, with information on the energy per photon lost.

5. Conclusion

We have shown that superconducting tunnel junctions based on niobium or hafnium may have considerable potential as photon counting optical and ultraviolet detectors. The basic experimental feasibility has now been demonstrated, and the

key features of such a detector can be summarised as follows: (a) photon counting operation with no readout noise, and with minimal dark current contribution; (b) an inherent spectroscopic capability at ultraviolet, optical, and infrared wavelengths, with tunnel noise-limited resolutions ranging from 0.4–4 nm at 100 nm and 5–50 nm at 500 nm for materials with T_c from $0.1 - 10$ K; (c) high quantum efficiency of 50 per cent or more over the range 100–2000 nm. A higher efficiency over a more restricted waveband could be achieved through the introduction of appropriate anti-reflection coatings; (d) high speed, limited primarily by the processing electronics, leading to a high count-rate capability, and high resolution time datation (sub-ms) of individual photon events; (e) inherent discrimination against background events through the application of energy and risetime discrimination.

An illustrative list of astronomical applications for which such a detector could play a major role, either at optical wavelengths from the ground ($\lambda > 350$ nm), or at ultraviolet and optical wavelengths ($\lambda \sim 100 - 2000$ nm) from space, would be: (a) faint object broad-band spectroscopy which, if coupled to a panoramic imaging capability, would lead to the direct determination of the spectral energy distribution and redshift of every object detected in the field either through the observation of continuum discontinuities (Lyman edge) or through the observation of line centroids; (b) highly efficient spectrophotometry of variable objects, with time resolution well below 1 ms; (c) order separation when coupling a strip of STJs to a high resolution echelle-type spectrograph; (d) speckle imaging, speckle spectroscopy, adaptive optics, interferometric fringe detection, and other atmospheric correction techniques requiring high time resolution.

An STJ array is already being considered as a possible European-contributed camera for Hubble Space Telescope (STECF 1995), and the benefits of the time and energy resolution for a space interferometer have also been considered (Perryman & Peacock 1995).

6. Acknowledgements

The authors acknowledge the technical support of A. van Dordrecht (ESTEC), R. Venn of Cambridge Microfab Ltd (UK) and D. Goldie of Oxford Instruments Ltd (UK).

References

Bardeen, J., Cooper, L., Schrieffer, J.R., 1957, Phys. Rev., 108, 1175.
Booth, N.E., 1987, Appl. Phys. Lett., 50, 293
Delamere, A., 1992, ESA SP-356, 111
Dravins, D., 1994, ESO Messenger, 78, 9
Fano, U., 1947, Phys. Rev., 72, 26
Giaever, I., 1960, Phys. Rev. Lett., 5, 464
Goldie, D.J., Brink, P.L., Patel, C., Booth, N.E., Salmon, G.L., 1994, Appl. Phys. Lett., 64, 3169
Gray, K., 1978, Appl. Phys. Lett., 32, 392
Josephson, B.D., 1962, Phys. Rev. Lett., 1, 251
de Korte, P.A.J., 1992, ESA SP-356, 41
Kurakado, M., 1982, Nucl. Instr. Meth., 196, 275
Lumb, D., van Dordrecht, A., Peacock, A., Rando, N., Verveer, J., Verhoeve, P., Goldie, D.J., Lumley, J., 1995, SPIE, 2518, 258
Morohashi, S., Imamura, T., Hasuo, S., 1992, J. Appl. Phys., 72, 7, 2969
Peacock, A., Verhoeve, P., Rando, N.,van Dordrecht, A., Erd, C., Perryman, M.A.C., Venn, R., Howlett, J., Goldie, D.J., Lumley, J., 1996a, Nature, In press
Peacock, A., Verhoeve, P., Rando, N.,van Dordrecht, A., Erd, C., Perryman, M.A.C., Venn, R., Howlett, J., Goldie, D.J., Lumley, J., 1996b, J. Appl. Phys., Submitted
Perryman, M.A.C., Foden, C.L., Peacock, A., 1993, Nucl. Instr. Meth. A325, 319
Perryman, M.A.C., Peacock, A., 1995, 'Future Possibilities of Astrometry from Space', ESA SP–379, 207
Petroff, M.D., Stapelbroeck, M.G., 1989, IEEE Trans Nucl. Sci., 36, 158
Rando, N., Peacock, A., van Dordrecht, A., Foden, C.L., Engelhardt, R., Taylor, B.G., Gare, P., Lumley, J., Pereira, C., 1992, Nucl. Instr. Meth., A313, 173
Rando, N., Verhoeve, P., van Dordrecht, A., Peacock, A., Perryman, M.A.C., Andersson, S., Verveer, J., 1996, Nucl. Instr. Meth., A370, 85.
STECF Newsletter No. 23, September 1995
Timothy, J., 1988, In 'Instrumentation for Ground-Based Optical Astronomy, Present and Future', ed. Robinson, L.B., Springer-Verlag, New York, 516
Verhoeve, P., Rando, N., Verveer, J., van Dordrecht, A., Peacock, A., Videler, P., Bavdaz, M., Goldie, D.J., Lederer, T., Scholze, F., Ulm, G., Venn, R., 1996, Phys. Rev. B., 53, 2, 809
Weast, R.C., ed., 1981, CRC Handbook of Chemistry and Physics, CRC Press Inc.
Weaver, J.H., Lynch, D.W., 1973, Phys. Rev. B, 7, 4311
Weaver, J.H., Krafka, C., Lynch, D.W., Koch, E.E., 1981, Physik Daten, 18-1
Wood, G.H., White, B., 1969, Appl. Phys. Lett., 15, 237

This article was processed by the author using Springer-Verlag TEX A&A macro package 1992.

FRONT ILLUMINATION BY OPTICAL PHOTONS FROM MONOCHROMATIC XENON LIGHT SOURCE

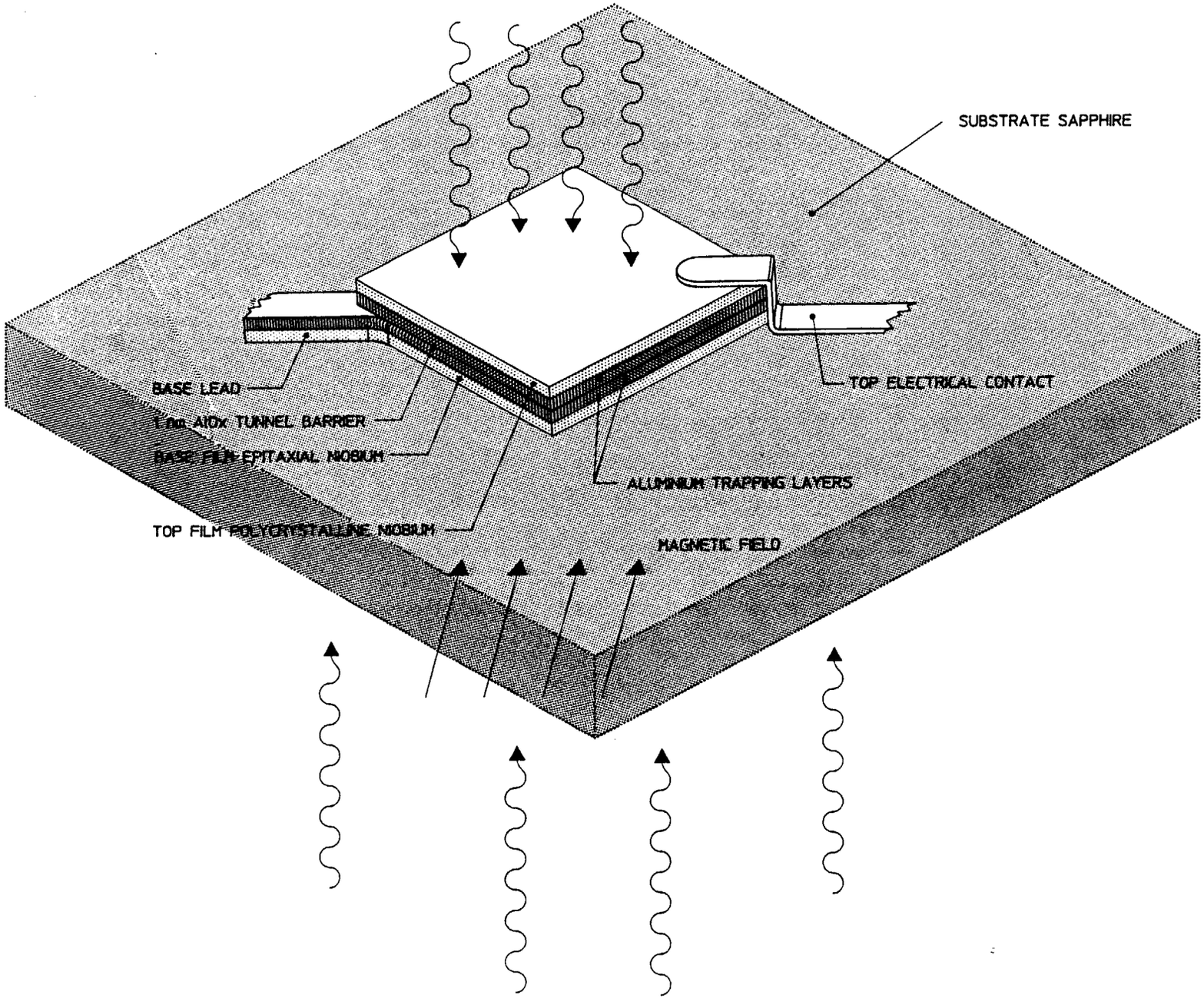

BACK ILLUMINATION MODE